

SEASONAL OCEANIC HEAT TRANSPORTS COMPUTED FROM AN ATMOSPHERIC MODEL AND OCEAN TEMPERATURE CLIMATOLOGY

THOMAS M. SMITH * and JAMES R. MILLER

*Department of Meteorology and Physical Oceanography, Cook College,
New Jersey Agricultural Experiment Station, Rutgers, The State University of New Jersey,
New Brunswick, NJ 08903 (U.S.A.)*

GARY L. RUSSELL

*NASA/Goddard Space Flight Center, Institute for Space Studies, 2880 Broadway, New York,
NY 10025 (U.S.A.)*

(Received August 4, 1987; revised September 2, 1988; accepted December 30, 1988)

ABSTRACT

Smith, T.M., Miller, J.R. and Russell, G.L., 1989. Seasonal oceanic heat transports computed from an atmospheric model and ocean temperature climatology. *Dyn. Atmos. Oceans*, 14: 77–92.

Seasonal estimates of the oceanic poleward heat transport are obtained using surface heat fluxes from a global atmospheric general circulation model on an $8^\circ \times 10^\circ$ grid and using rates of ocean heat storage to 1500 m calculated from the seasonal climatological ocean temperature data of Levitus. The rate of change of heat storage in the deep ocean (below 1500 m) is assumed to be spatially uniform. The global oceanic meridional transports for each latitude are calculated. The results are compared with those of Russell et al., in which seasonal ocean transports were calculated using the same method except that in that study the rate of change of heat storage was calculated using observed surface temperatures and mixed-layer depths. In the present study, the maximum meridional transports are about the same magnitude, but shifted to earlier in the year; the transports are near zero outside the band between 30°N and 30°S and no secondary maximum of northward transports occurs in the Southern Hemisphere in the first half of the year. The use of the Levitus seasonal temperature data to calculate heat storage to 1500 m did not reduce the amplitude of the annual rate of heat storage change in the deep ocean below the 11 W m^{-2} value obtained by Russell et al. The amplitude, however, was reduced by about half when the calculations were redone using the Levitus temperature data only down to 300 m. Sensitivity studies were carried out to assess the effects of errors in the Levitus temperature climatology on the ocean heat transports. The sparse data in the Southern Hemisphere caused larger errors in the Southern Hemisphere transports.

* Present address: College of Marine Studies, University of Delaware, Lewes, DE.

1. INTRODUCTION

The poleward transport of heat by the atmosphere and ocean is necessary to maintain the global heat balance of the Earth. Knowledge of these transports is important for understanding the global climatic system. Ocean heat transports have been calculated using several different methods as described by Bryan (1982).

The indirect method for calculating annual ocean heat transports uses surface heat fluxes across the air-sea interface and the assumption that there is no net oceanic heat storage over an annual cycle. Hastenrath (1982) and Hsiung (1985) have used observed fluxes, and Slingo (1982) and Miller et al. (1983) have used fluxes generated by an atmospheric general circulation model (GCM) to determine annual heat transports.

Russell et al. (1985, hereafter referred to as RMT) used the indirect method to calculate seasonal ocean heat transports by assuming that changes in ocean heat storage could be determined from climatological sea-surface temperatures and mixed-layer depths. The purpose of this paper is to extend the results of RMT by using the seasonal ocean temperature climatology of Levitus (1982,1984) to more accurately determine changes in ocean heat storage. The surface heat fluxes are the same as those in RMT. The results from this study are compared with those of RMT and with other studies. Relative error estimates of the transports as a function of latitude are also discussed.

2. CALCULATION OF THE SEASONAL OCEANIC HEAT TRANSPORT

The seasonal northward transport of heat across a particular latitude is obtained by integrating the converged horizontal ocean heat transport from that latitude to the North Pole. For each 8° by 10° GCM grid box (latitude and longitude, respectively), the converged ocean heat transport OT is calculated by

$$OT = \frac{\partial EU}{\partial t} + \frac{\partial ED}{\partial t} - VF \quad (1)$$

where VF is the surface heat flux and EU and ED are ocean heat storage in the upper and deep ocean, respectively.

The surface heat fluxes, which are the same as those used in RMT, are obtained from the version of the atmospheric GCM of Hansen et al. (1983), in which each grid box is either all land or all ocean. The vertical flux is given each day at each grid box and is fit with a Fourier series using the mean and first harmonic. The upper ocean heat storage is calculated by the equation

$$EU = \rho_w C_w \int_{-h}^0 T(z) dz + \rho_l Z_1 [-L + C_l T_l - C_w T(0)] \quad (2)$$

where ρ_w and ρ_i are the densities of water and ice, C_w and C_i the specific heats of water and ice, h the depth of the upper ocean, T the water temperature, T_i the ice temperature, Z_i the ice depth and L the latent heat of melting. The difference between this study and that of RMT is in the calculation of the integral in eqn. (2). In RMT, the integral was calculated by using climatological sea-surface temperatures and mixed layer-depths and assuming that the depth of the upper ocean was the depth of the annual-maximum mixed layer at each grid box. In the present study, the integral is calculated to a depth of 1500 m using the ocean temperature climatology of Levitus (1982).

The ocean temperature data are obtained from the seasonal ocean temperature climatology compiled by Levitus (1982) from National Oceanographic Data Center records covering the period from 1900 to 1978. The climatology gives temperatures in a $1^\circ \times 1^\circ$ grid at each of 24 layers from the surface to 1500 m depth. Where there are no observations, temperatures are assigned by horizontal interpolation from nearby values. It is significant that in the Southern Hemisphere data is scarce, and extensive interpolation is employed.

The ocean energy is calculated on the 1° grid using eqn. (2) for each season, defined in the Levitus data as February–April, May–July, August–October and November–January. The energy calculation includes the effects of ice and snow, with ice amounts specified from Alexander and Mobley (1976), and Walsh and Johnson (1979). The seasonal energy is then interpolated to an $8^\circ \times 10^\circ$ grid. Figure 1 shows seasonal energy differences, August–October minus February–April, for the surface to 300-m layer and the 1200-m to 1500-m layer. Interesting features in the surface layer include the area of positive differences in the tropical Pacific Ocean, in the Gulf Stream region extending to the north of Iceland, and in the Kuroshio Current region. In the 1200-m to 1500-m layer, the Northern Hemisphere shows almost no energy differences except in the Gulf Stream region. The Southern Hemisphere shows large unexplained maxima and minima in all layers down to 1500 m, and it is believed that the existence of only a few observations is responsible.

To calculate ocean heat transports, the ocean energy is first fitted with a quadratic spline, and then smoothed with the zeroth and first harmonics of the Fourier series at every ocean location. As in RMT, the rate of change of heat storage in the deep ocean must also be calculated to find seasonal ocean heat transports. If eqn. (1) is averaged over the globe, we obtain

$$0 = \frac{\partial \overline{EU}}{\partial t} + \frac{\partial \overline{ED}}{\partial t} - \overline{VF} \quad (3)$$

where the overbar denotes a global average and the left-hand side is zero

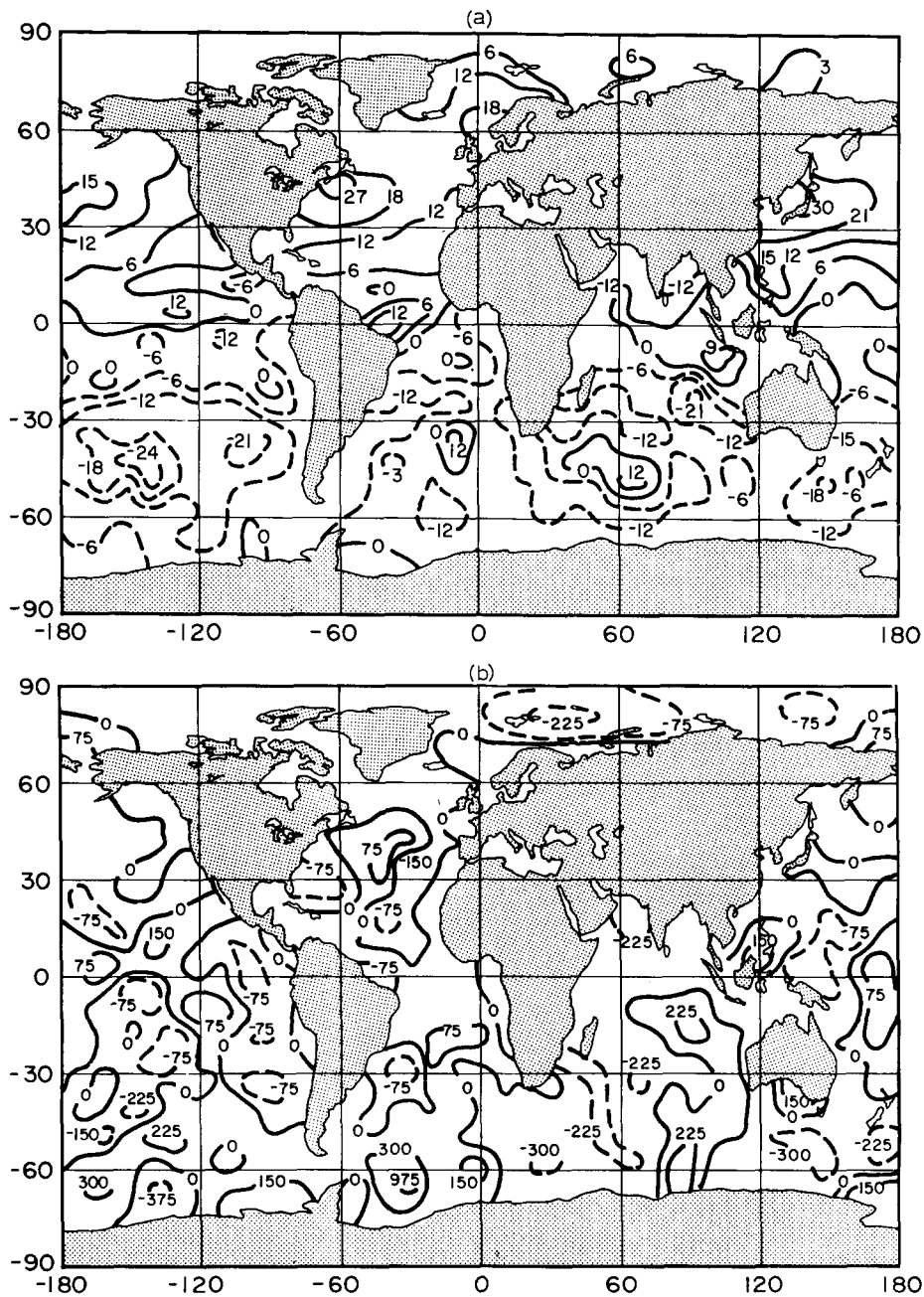


Fig. 1. Seasonal differences (August–October less February–April) in ocean thermal energy in 300-m layers from the surface to a depth of 1500m: (a) 0–300 m, units are 10^8 J m^{-2} ; (b) 1200–1500 m, units are 10^6 J m^{-2} .

because the global average of the ocean heat transport is zero. The global average rate of change of heat storage in the deep ocean is then determined by calculating the other two terms in eqn. (3) from the ocean temperature climatology and the surface heat fluxes. The same assumption as used by RMT, that the rate of change of heat storage in the deep ocean is spatially uniform, is then used to obtain

$$OT = \frac{\partial EU}{\partial t} + \frac{\partial \overline{ED}}{\partial t} - VF \quad (4)$$

As the depth of the upper ocean increases, the rate of change of heat storage in the deep ocean should decrease. The use of the climatological ocean temperature data to a depth of 1500 m for the upper ocean should lead to more accurate heat transports than those obtained by RMT. The converged transport is then integrated from latitude ϕ to the North Pole to obtain

$$Q_\phi = \int_\phi^{90^\circ N} OT \cdot dA \quad (5)$$

where Q_ϕ is the northward transport of heat across latitude ϕ .

3. SEASONAL CHANGES IN MERIDIONAL OCEANIC HEAT TRANSPORT

Equations (4) and (5) are used to calculate the northward oceanic heat transport across each latitude. Figure 2 shows the northward oceanic heat transport with the upper ocean specified as 1500 m deep and comparisons with the seasonal calculations of RMT for each quarter. The maximum northward and southward global transports in the first quarter occur near the same latitude in each study. However, the maximum global northward and southward transports have increased to 7.5 and 2.2 PW respectively, as compared with 5 and 0.5 PW respectively in RMT (1 PW = 10^{15} W).

In general, the principal difference between the present study and RMT is that, by using the Levitus temperature climatology to calculate changes in oceanic heat storage, the maximum northward transports are larger than in RMT in the first, third and fourth quarters and are smaller than RMT in the second quarter. The latitudes at which the maximum northward transports occur are similar in both studies. One major difference occurs in the second quarter, since the present study shows a slight southward global transport in the Southern Hemisphere in contrast to the relatively large northward global transport in RMT.

Figure 2 shows that there is a systematic difference in the transports in the second and fourth quarters. For the present study, the northward transports are smaller at all latitudes in the second quarter and larger at all latitudes in the fourth quarter when compared with RMT. Since the surface

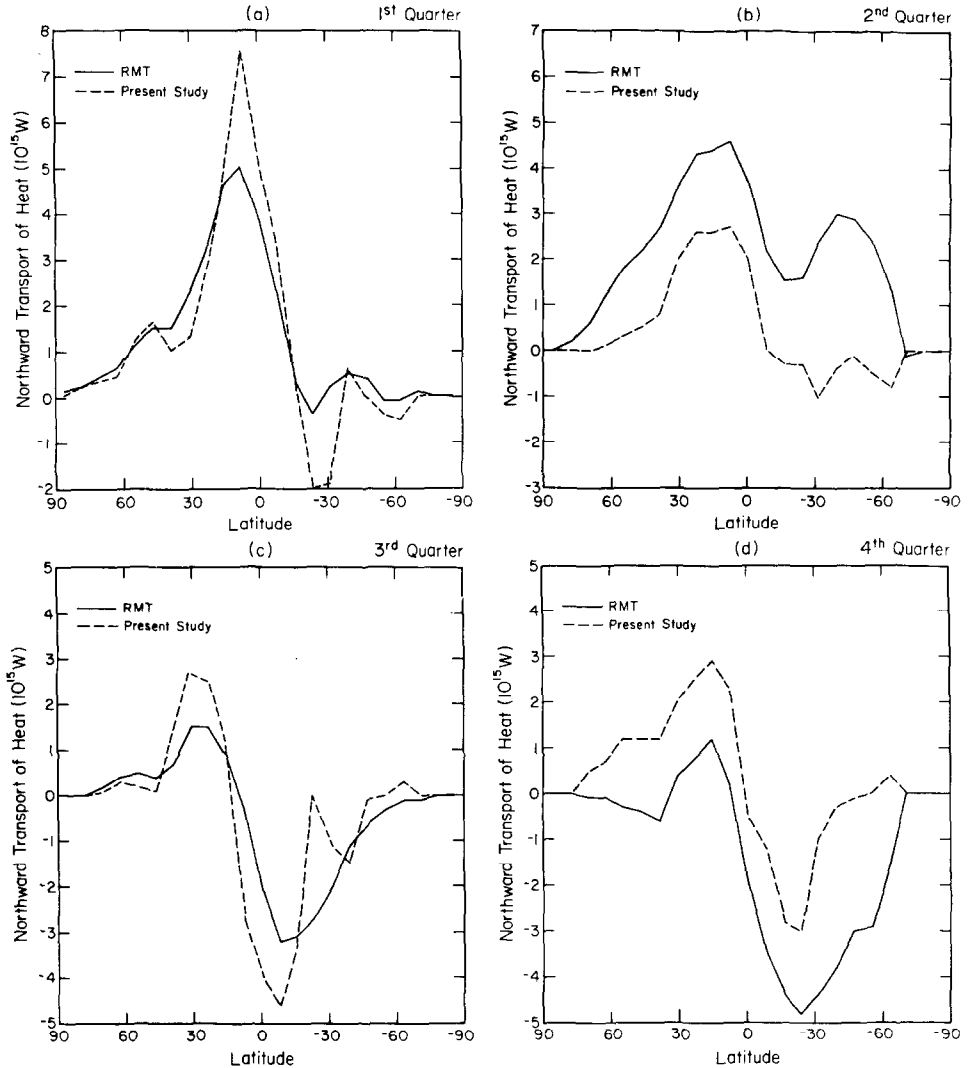


Fig. 2. Quarterly northward ocean heat transports from the present study and from Russell et al. (1985) for (a) the first, (b) second, (c) third, (d) fourth quarter.

heat fluxes are the same in both studies, the differences must be due to the ocean heat storage.

Figure 3 shows the latitudinal variation of the annual cycle of the rate of heat storage for RMT and for the present study. Although there appears to be a small phase shift between the two studies, the principal difference is that the maxima occur at higher latitudes in RMT. Hence, the positive rate of heat storage in the second quarter north of 50°N in RMT requires a

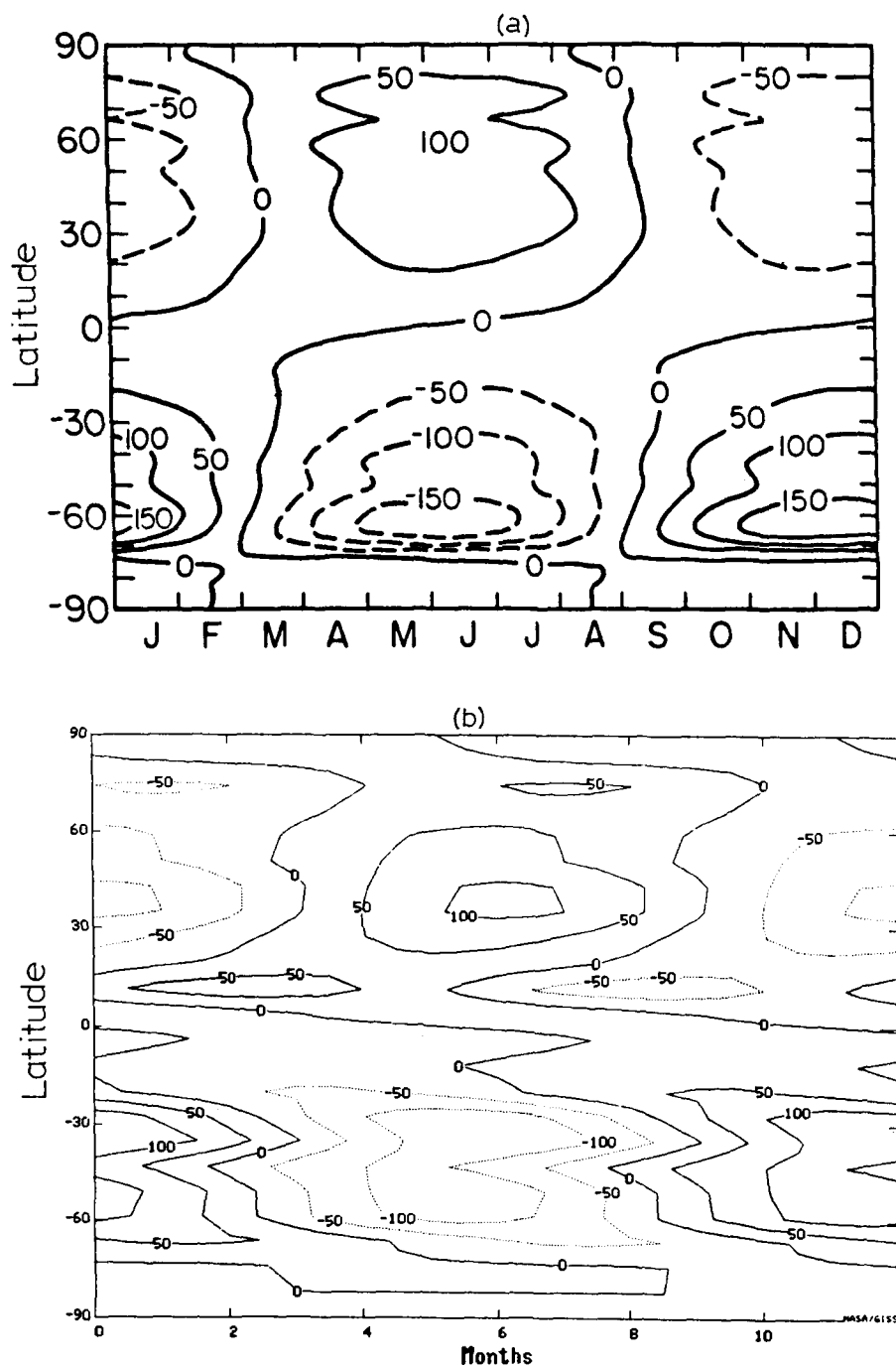


Fig. 3. Annual cycle of rate of heat storage (W m^{-2}) for (a) RMT and (b) for the present study to a depth of 1500 m.

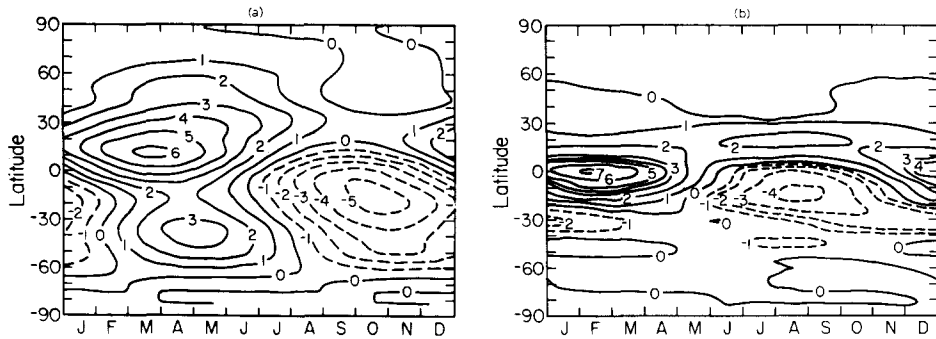


Fig. 4. Annual variation of heat transports (PW) from (a) Russell et al. (1985) and (b) the present study.

northward transport into that region and, therefore, northward heat transport at all latitudes in the Northern Hemisphere. In the Southern Hemisphere a small southward transport of heat is required to balance the surface heat fluxes in the present study. The much larger rate of heat storage decrease in RMT for the high latitudes of the Southern Hemisphere requires that heat be transported away toward lower latitudes, which leads to a net northward heat transport in the second quarter for the Southern Hemisphere.

In the fourth quarter the larger rate of heat storage decrease at high northern latitudes in RMT means that less northward transport is required. In the Southern Hemisphere the larger increase in rate of heat storage at high latitudes in RMT requires more southward heat transport. Hence the curve for the northward heat transport in RMT in Fig. 3 is always below the curve for the present study in the fourth quarter. The shift of the maxima in Fig. 3 to higher latitudes in RMT, particularly near 60°S , is likely to be due to the way the annual cycle of mixed-layer depths is specified there.

The differences between the present study and RMT can be seen more clearly in Fig. 4, which shows the annual variation of the global transports as a function of latitude. The maximum northward transport has increased slightly from 6 to 7 PW, but the location of the maximum has shifted to the south and to earlier in the year. The maximum southward transport in the second half of the year has decreased from 5 to 4 PW and also shifted to earlier in the year. The temporal shift in the location of the maximum northward transport accounts for the seasonal transport differences in the first and second quarters in Fig. 2. In the RMT study, the first and second quarter maxima are about the same because the maximum occurs between the two seasons. The shift of the maximum toward the first quarter in the present study accounts for the increase in transports in the first quarter and

decrease in the second quarter as compared with RMT in Fig. 2. Hence, the significant changes in magnitude in Fig. 2 are primarily due to the phase shift.

Figure 4 shows the second major difference from RMT shown in Fig. 2, namely the disappearance of the large northward transport at 40°S in the second quarter shown in RMT. The only difference between the two studies is in the calculation of the oceanic heat storage. At 40°S there is a near balance between the surface heat flux and the change in heat storage in the present study. In RMT, the rate of heat storage increase was greater and therefore required an inflow of heat into the region.

The third major difference in the present study is that the transport is confined primarily to the band between 30°N and 30°S . The RMT study showed that although the maximum transports were confined to the same band, there were significant transports of 1–2 PW poleward of 30° in both hemispheres. This implies that the incoming surface heat flux nearly balances the change in heat storage poleward of 30° in the present study, and that there is a greater amount of heat storage at the higher latitudes in the winter hemisphere in the RMT study.

Figure 5 shows the annual variations of global oceanic heat transport calculated by Oort and Vonder Haar (1976) using the residual method and calculated by Meehl et al. (1982) using a numerical ocean model. The magnitude of the maximum northward transports are about the same but the maximum southward transport of 4 PW in the present study is about half that of the other two studies. There is also a shift in phase, with the maximum northward transport occurring earlier in the year in the present study. The study of Meehl et al. also shows larger transports poleward of 30° , particularly in the Southern Hemisphere.

The difference between this study and that of RMT is in the calculation of the upper ocean heat storage. In both studies it is assumed that the rate of change of heat storage in the deep ocean is spatially uniform. This assumption is potentially more critical in RMT because the upper ocean depth is at most 250 m. The calculations of RMT showed that the global imbalance of surface heat flux and upper ocean heat storage produced an annual variation of heat storage in the deep ocean with an amplitude of 11 W m^{-2} . It was assumed that using the Levitus temperature climatology to a depth of 1500 m would significantly decrease the amplitude of the annual variation of heat storage in the deep ocean, since the upper ocean would now be 1500 m deep as opposed to the shallower depth in RMT. The calculations, however, showed that the amplitude was still about 11 W m^{-2} .

The most likely reason for the still significant flux of heat into the deep ocean below 1500 m is the presence of significant errors in the ocean temperature climatology in the Southern Hemisphere. This occurs because

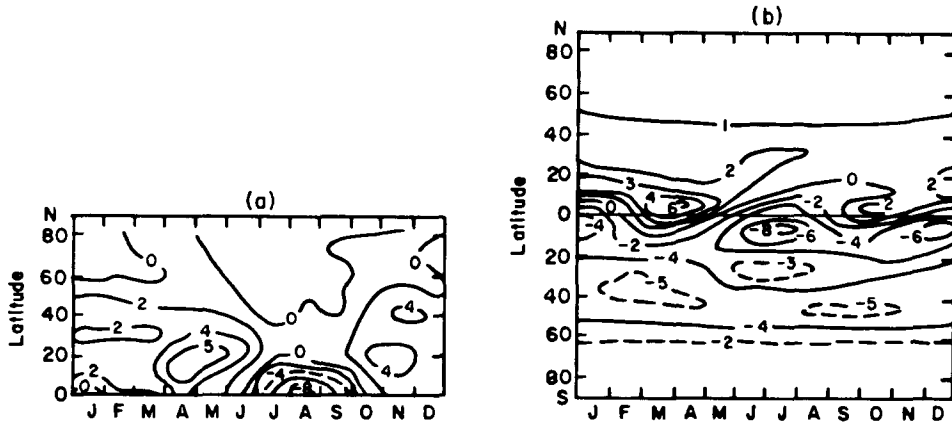


Fig. 5. Annual variation of heat transports (PW) from (a) Oort and Vonder Haar (1976) for the Northern Hemisphere, and (b) Meehl et al. (1982); from Russell et al. (1985).

of the sparse data in the Southern Hemisphere, particularly at the deeper depths. As a check on this hypothesis the ocean heat transports were recalculated using the climatological temperatures, but using different depths for the upper ocean. When the upper ocean was taken as 300 m, the amplitude of the deep ocean heat storage was reduced to 6 W m^{-2} . This tends to support the idea that the calculation of oceanic heat storage is less accurate at the deeper depths, although errors in the surface heat fluxes might also account for some of the change between the 300-m and 1500-m calculations. Figure 6 shows the ocean heat transports for the 300-m-deep upper ocean. The pattern is similar to Fig. 4b but there are slightly stronger transports poleward of 30° .

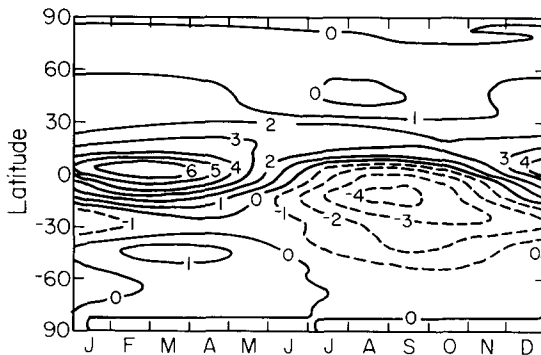


Fig. 6. Annual variation of heat transports (PW) when the depth of the upper ocean is taken as 300 m in the present study.

Although the flux of heat into the Southern Hemisphere deep ocean below 1500 m is likely to be due to errors in the temperature climatology, the 300-m layer may be too shallow. Levitus (1984) shows that there is a large annual temperature cycle in the 40–60°S latitude belt down to 1000 m. Since data are sparse in this region, it is difficult to know whether the annual variation at these depths is realistic.

4. SENSITIVITY STUDIES

Errors in the Levitus ocean heat storage occur in some Southern Hemisphere locations where there are few data, and large maxima or minima occur in the ocean energy difference field as shown in Fig. 1. Because a small temperature error can produce a large energy error when integrated over a 1500-m layer, the lack of Southern Hemisphere temperature observations may be responsible for significant ocean energy errors. A uniform error of 1°C over a 1500-m-deep column of water produces a heat storage error of $6 \times 10^9 \text{ J m}^{-2}$. Over an $8^\circ \times 10^\circ$ grid box, with a mid-latitude area of $6 \times 10^{11} \text{ m}^2$, and over one season, the associated error in converged horizontal heat transport is about 0.6 PW. Although actual errors are likely to be much smaller than 1°C, there are hundreds of grid boxes in which errors may exist.

The quality of the oceanic and atmospheric data are critical in determining the accuracy of the seasonal poleward heat transports. The atmospheric vertical heat fluxes are determined by an atmospheric GCM. It is difficult to determine the maximum magnitude and distribution of errors in the vertical heat fluxes. A detailed study of surface heat fluxes in areas where there is a high density of observations would quantify the model's error in these areas. Model errors could then be incorporated into sensitivity studies. Because model-generated vertical heat flux errors have not been studied adequately, they are not considered in the following sensitivity studies.

The method used for assessing the effect of errors in the ocean temperature climatology on the ocean heat transports was to insert random errors into the temperatures at each grid box. Although a different random error could be inserted in each ocean grid box, the following analysis will assume that the variance of the errors is the same at each grid box for a particular latitude band. Different latitudes, however, may be assigned different variances. The transport error across a particular latitude will be determined by first rewriting eqn. (5) and then calculating its standard deviation as a function of the temperature standard deviation in the upper ocean. By assuming that the standard deviation of temperature corresponds to the errors in the temperature climatology, the corresponding transport errors are obtained.

The northward heat transport across latitude ϕ can be rewritten from eqn. (5) as

$$Q_\phi = \int_\phi^{90^\circ\text{N}} \left(\frac{\partial EU}{\partial t} - \frac{\partial \overline{EU}}{\partial t} \right) dA - \int_\phi^{90^\circ\text{N}} (VF - \overline{VF}) dA \quad (6)$$

Since

$$\frac{\partial \overline{EU}}{\partial t} = \frac{1}{A} \left(\int_\phi^{90^\circ\text{N}} \frac{\partial EU}{\partial t} dA + \int_{90^\circ\text{S}}^\phi \frac{\partial EU}{\partial t} dA \right) \quad (7)$$

where A is the global ocean area, eqn. (6) can be rewritten as

$$Q_\phi = \left(1 - \frac{A_\phi}{A} \right) \int_\phi^{90^\circ\text{N}} \frac{\partial EU}{\partial t} dA - \frac{A_\phi}{A} \int_{90^\circ\text{S}}^\phi \frac{\partial EU}{\partial t} dA - \int_\phi^{90^\circ\text{N}} (VF - \overline{VF}) dA \quad (8)$$

where A_ϕ is the ocean area north of latitude ϕ . The purpose of writing the transports in the form used in eqn. (8) is that there is a simple direct dependence of the transports on the upper ocean energy at any given location. When calculating the variance of the transports, the variance of the surface heat flux is assumed to be zero. With this assumption, eqn. (8) can be used to calculate the variance of the transport at any time or integrated over time to yield an average over any desired period. By integrating eqn. (8) over a period of time Δt equal to one season and then taking the variance yields

$$\begin{aligned} \text{var}(Q_\phi)_s = \frac{1}{\Delta t^2} & \left\{ \left(1 - \frac{A_\phi}{A} \right)^2 \text{var} \left[\int_\phi^{90^\circ\text{N}} (E_2 - E_1) dA \right] \right. \\ & \left. + \left(\frac{A_\phi}{A} \right)^2 \text{var} \left(\int_{90^\circ\text{S}}^\phi (E_2 - E_1) dA \right) \right\} \quad (9) \end{aligned}$$

where $(Q_\phi)_s$ is the seasonal average of Q_ϕ , and E_1 and E_2 represent the thermal energy at the beginning and end of the time period Δt .

The integrals in eqn. (9) are calculated by assuming that the temperatures in different layers and in different grid boxes are independent and by summing over latitude bands to obtain

$$\begin{aligned} \text{var}(Q_\phi)_s = \frac{2}{\Delta t^2} & \left[\left(1 - \frac{A_\phi}{A} \right)^2 \sum_{j=\phi}^{\text{NP}} \sum_{k=1}^K \sum_{i=1}^{n_j} \text{var}(\rho_w C_w T_{i,j,k}) \Delta z_k^2 B_j^2 \right. \\ & \left. + \left(\frac{A_\phi}{A} \right)^2 \sum_{j=\text{SP}}^\phi \sum_{k=1}^K \sum_{i=1}^{n_j} \text{var}(\rho_w C_w T_{i,j,k}) \Delta z_k^2 B_j^2 \right] \quad (10) \end{aligned}$$

where NP and SP are the North and South Poles, K is the number of temperature layers, n_j is the number of grid boxes at latitude j , $T_{i,j,k}$ is the mean temperature of a grid box at layer k , Δz_k is the thickness of layer k , and B_j is the area of a grid box at latitude j . If we let

$$\sigma_{H,j}^2 = \sum_{k=1}^K \sum_{i=1}^{n_j} \text{var}(\rho_w C_w T_{i,j,k}) \Delta z_k^2 B_j^2 \quad (11)$$

be the variance of the heat storage for latitude band j , then eqn. (10) becomes

$$\text{var}(Q_\phi)_s = \frac{2}{\Delta t^2} \left[\left(1 - \frac{A_\phi}{A}\right)^2 \sum_{j=\phi}^{\text{NP}} \sigma_{H,j}^2 + \left(\frac{A_\phi}{A}\right)^2 \sum_{j=\text{SP}}^{\phi} \sigma_{H,j}^2 \right] \quad (12)$$

The errors in the temperature climatology of Levitus (1982) have not been calculated. For a particular grid box the standard error of temperature can be calculated as the standard deviation of the temperature divided by the square root of the number of observations in the grid box. Since the data necessary to make this calculation were not available, the standard deviation of heat storage by 5° latitude bands given in Levitus (1984) was used in eqn. (12) rather than use temperature standard errors. Levitus (1984) sums over 1° squares to obtain the seasonal values of the standard deviation of heat storage in a 275-m layer by 5° latitude bands for the global ocean. The values for the Northern Hemisphere winter season were inserted for $\sigma_{H,j}^2$ in eqn. (12). Since the standard errors would be smaller than these values, we obtain an upper bound on the errors in the ocean heat transport.

The solid curve in Fig. 7 shows the variation of the transport errors by latitude due to the errors in the ocean heat storage. The maximum error occurs at the Equator. Since the Southern Hemisphere contains more ocean than the Northern Hemisphere, one would expect the maximum error to be in the Southern Hemisphere. This does not occur because the larger area in the Southern Hemisphere is offset by somewhat larger standard deviations in the Northern Hemisphere.

Since there was considerable variability in the number of observations that were available for each grid box in constructing the ocean temperature climatology, the climatology is much more reliable at some grid boxes than at others. There are more observations in the Northern Hemisphere than in the Southern Hemisphere. The average number L_j of observations at 300 m in a 5° grid box was calculated for each latitude band from the data of Levitus (1982). The value of $\sigma_{H,j}^2$ in eqn. (12) was then replaced by $C \cdot \sigma_{H,j}^2 / L_j$ to obtain a new estimate of the transport errors. The value of the constant C is chosen so that the sum of $\text{var}(Q_\phi)$ over all latitude bands is the same as for the solid curve in Fig. 7.

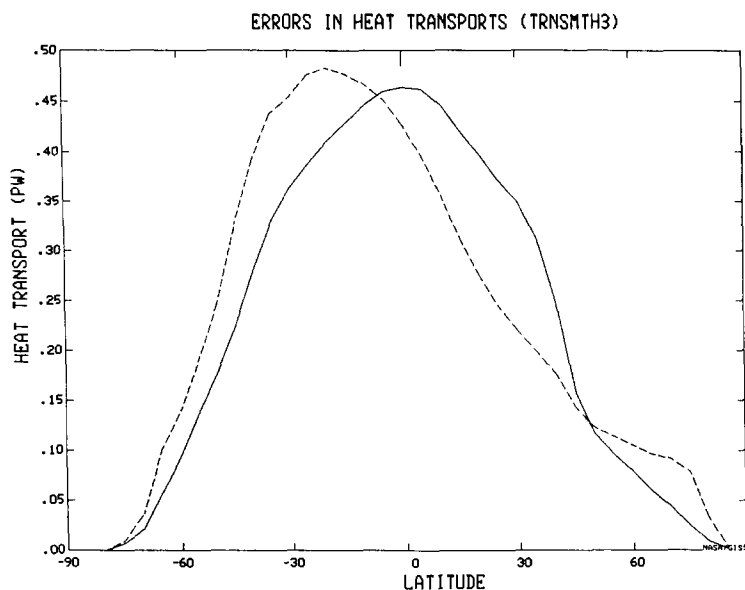


Fig. 7. Solid curve is the upper bound on the ocean heat transport error for a 275-m-deep ocean as calculated from the Levitus (1984) standard deviations of heat storage for 5° latitude bands. Dashed curve shows the error when weighted by average number of observations per grid box for each latitude band.

The dashed curve in Fig. 7 shows the transports when the errors depend on the number of observations in each latitude band. The latitude at which the maximum error occurs shifts toward the Southern Hemisphere and the error at 30°S is now more than twice as large as the error at 30°N . Although the absolute errors given in Fig. 7 provide upper bounds on the errors, the relative errors due to the sparsity of the data in the Southern Hemisphere are apparent. This study could be extended by inserting errors into each ocean grid box instead of by latitude bands and calculating more accurate values of the standard errors of temperature. The study should also be extended to deeper depths so that transport errors that arise owing to neglect of actual deep ocean heat storage changes can be eliminated.

5. SUMMARY

Seasonal poleward heat transports in the ocean were calculated using the Goddard Institute of Space Studies (GISS) atmospheric GCM for surface heat fluxes and the Levitus (1982) ocean temperature climatology to compute ocean heat storage. This study uses the same vertical heat fluxes as RMT. It differs from RMT by using an ocean temperature climatology which extends from the surface to 1500 m, rather than using the climatologi-

cal sea-surface temperature and mixed-layer depths. The present study computed the ocean heat storage directly, where RMT assumed the ocean temperature was constant from the surface to the bottom of the mixed layer in order to compute the mixed-layer heat storage. The maximum transports are 7 PW northward in February and 4 PW southward in August. The transports are confined almost entirely to the band between 30°N and 30°S latitude. Compared with RMT, the transports are stronger in the first half of the year, weaker in the second half, and more confined to the equatorial region. These transports also contain no secondary maximum in the Southern Hemisphere as found in RMT.

The effects of errors in the ocean temperature climatology on the heat transports were also examined. Although there are also errors in the heat fluxes obtained from the atmospheric model, their effects were not considered. The sensitivity of the ocean heat transports to temperature errors in the upper 275-m layer was evaluated by inserting the standard deviations of heat storage as calculated by Levitus (1984). When the errors were modified based on the number of observations per latitude band, the latitude at which the maximum transport error occurred shifted southward to about 20°S . The transport errors were more than twice as large at 30°S as at 30°N .

The principal goal of this research was to extend the results of RMT by using a more accurate calculation of the ocean heat storage using the ocean temperature climatology of Levitus (1982). By calculating the heat storage to a depth of 1500 m, it was expected that the amplitude of the annual rate of heat storage in the deep ocean would be reduced from the 11 W m^{-2} in RMT. This did not occur, however, and since the use of the climatological data to 300 m depth did reduce the deep ocean rate from 11 to 6 W m^{-2} , it may be that the sparse data in the deeper (300–1500 m) layers of the Southern Hemisphere, may have prevented more improvement over the RMT study. Future studies using the climatological data might be better if confined to the upper 300-m layer.

ACKNOWLEDGMENTS

The authors would like to thank T. Kuczek for help in formulating the statistical expression for variance, D. Hoehler for help with computer programming and S. Levitus for a discussion of the temperature errors.

REFERENCES

- Alexander, R.C. and Mobley, R.L., 1976. Monthly average sea-surface temperature and ice-pack limits on a 1 deg global grid. *Mon. Wea. Rev.*, 104: 143–148.
- Bryan, K., 1982. Poleward heat transport by the ocean: observations and models. *Ann. Rev. Earth Planet Sci.*, 10: 15–38.

- Hansen, J., Russell, G., Rind, D., Stone, P., Lacis, A., Lebedeff, S., Ruedy, R. and Travis, L., 1983. Efficient three-dimensional global models for climate studies: models I and II. *Mon. Wea. Rev.*, 111: 609–662.
- Hastenrath, S., 1982. On meridional heat transports in the world ocean. *J. Phys. Oceanogr.*, 12: 922–927.
- Hsiung, J., 1985. Estimates of global oceanic meridional heat transport. *J. Phys. Oceanogr.*, 15: 1405–1413.
- Levitus, S., 1982. Climatological Atlas of the World Ocean. NOAA, Prof. pap. 13, U.S. Govt. Printing Office, Washington, DC, 173 pp.
- Levitus, S., 1984. Annual cycle of temperature and heat storage in the world ocean. *J. Phys. Oceanogr.*, 14: 727–746.
- Meehl, G.A., Washington, W.M. and Semtner, A.J., 1982. Experiments with a global ocean model driven by observed atmospheric forcing. *J. Phys. Oceanogr.*, 12: 301–312.
- Miller, J.R., Russell, G.L. and Tsang, L.-C., 1983. Annual oceanic heat transports computed from an atmospheric model. *Dyn. Atmos. Oceans*, 7: 95–109.
- Oort, A.H. and Vonder Haar, T.H., 1976. On the observed annual cycle in the ocean-atmosphere heat balance over the Northern Hemisphere. *J. Phys. Oceanogr.*, 6: 781–800.
- Russell, G.L., Miller, J.R. and Tsang, L.-C., 1985. Seasonal oceanic heat transports computed from an atmospheric model. *Dyn. Atmos. Oceans*, 9: 253–271.
- Slingo, J.M., 1982. Study of the Earth's radiation budgets. *Q.J.R. Meteorol. Soc.*, 108: 379–405.
- Walsh, J. and Johnson, C., 1979. An analysis of Arctic sea ice fluctuations. *J. Phys. Oceanogr.*, 9: 580–591.